Electronic Supplementary Material (ESI) for Green Chemistry.

A glucose tolerant β-Glucosidase from *Thermomicrobium roseum* that can hydrolyze biomass in seawater

Sushant K. Sinha[*,a], *Maithili Datta*[a], *and Supratim Datta*[* a,b,c]

[a] Protein Engineering Laboratory, Department of Biological Sciences, Indian Institute of Science Education and Research Kolkata, Mohanpur, West Bengal

[b]Center for the Advanced Functional Materials, Indian Institute of Science Education and Research Kolkata, Mohanpur, West Bengal

[c]Center for the Climate and Environmental Sciences, Indian Institute of Science Education and Research Kolkata, Mohanpur, West Bengal

*Corresponding author: Sushant K. Sinha, Supratim Datta, Department of Biological Sciences, Indian Institute of Science Education and Research Kolkata Mohanpur 741246, West Bengal, India.; email: sushantkrsinha13@gmail.com or supratim@iiserkol.ac.in

Materials and Methods:

Homology modeling: The B9L147 structure was generated by homology modeling in the SWISS-MODEL server. The GH1 β-glucosidase template from TD2F2 (PDB Id: 3wh5, sequence identity 59.6%, GMQE 0.76) was used to obtain B9L147 model. The built model quality of B9L147 satisfied the quality thresholds of the program. Further, the B9L147 model was examined for stereo-chemical quality and fold quality using online tools PROCHECK and ProSA[1,2]. The Z-score value of the B9L147 model is -9.82, which is in the distribution range of the protein chains of similar size in the PDB database, indicating the built model of B9L147 is suitable for structural analysis.

HPLC analysis of B9L147 reaction product: The hydrolysis product of cellobiose with and without exogenously added glucose monitored by HPLC. The reaction product contains 50 mM of cellobiose, 1 µg B9L147 enzyme, and 100 mM of glucose, assayed for 10 min at 84 °C and heat-inactivated at 95 °C for 5 min. The reaction product was centrifuged for 15 min at 13000 rpm and then analyzed by HPLC. In HPLC analysis, the mobile phase is acetonitrile and water in a 3:1 ratio and 3.9 X 300 mm Waters carbohydrate analysis column used for separation using a Water's HPLC system (Waters Corp., Milford, MA, USA), with an evaporative light scattering (ELS) detector.

Cloning, expression, and purification of endoglucanase CBP-105: The synthetic gene corresponding to the GH9 endoglucanase from *Cellulomonas flavigena* was constructed and assembled by Gene Art (Thermo Fisher Scientific, Waltham, USA). The CBP-105 gene was cloned into a T7 based bacterial plasmid and expressed in E. coli BL21(DE3) expression strain. For enzyme expression, the cells were grown at 37 °C in LB media with antibiotic ampicillin (100 µg/mL) and induced with 0.5 mM IPTG for an additional 5 h at 37 °C. Cells were harvested by centrifugation at 8000×g for 10 min at 4 °C. For purification, we followed the same procedure as described in the method section of the main paper.

Figure S1. Molecular weight and purity of His trap column purified B9L147 protein on SDS-PAGE (10%). Lane M: PageRuler™ Prestained Protein Ladder, Thermo Fisher Scientific (Waltham, USA), while in lane B9L147, purified B9L147 protein band after the Ni-NTA purification (apparent molecular weight 52 kDa).

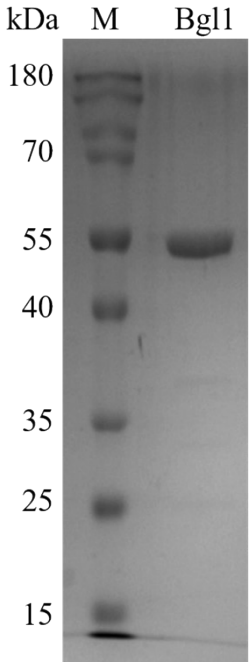

Figure S2. Structure-based multiple sequence alignment of B9L147 with glucose tolerant GH1 BGs. The secondary structure of the proteins was generated using the ESPript algorithm[3]. The arrow above the sequence represents β-sheets, while the spiral lines indicate α- helices. The proteins chosen were B8CYA8[4]: *Halothermothrix orenii* (100 % activity at 1.4 M glucose), Td2f2[5]: bacterium metagenome ($IC_{50,Glc} > 1$ M), O08324[6]: *Thermococcus* sp. (100 % specific activity up to 4 M glucose), A0A0F7KKB7[7]: bacterial metagenome ($IC_{50,Glc} = 3.5$ M), D5KX75[8]: Marine microbial metagenome ($K_{i,Glc} = 1000$ mM).

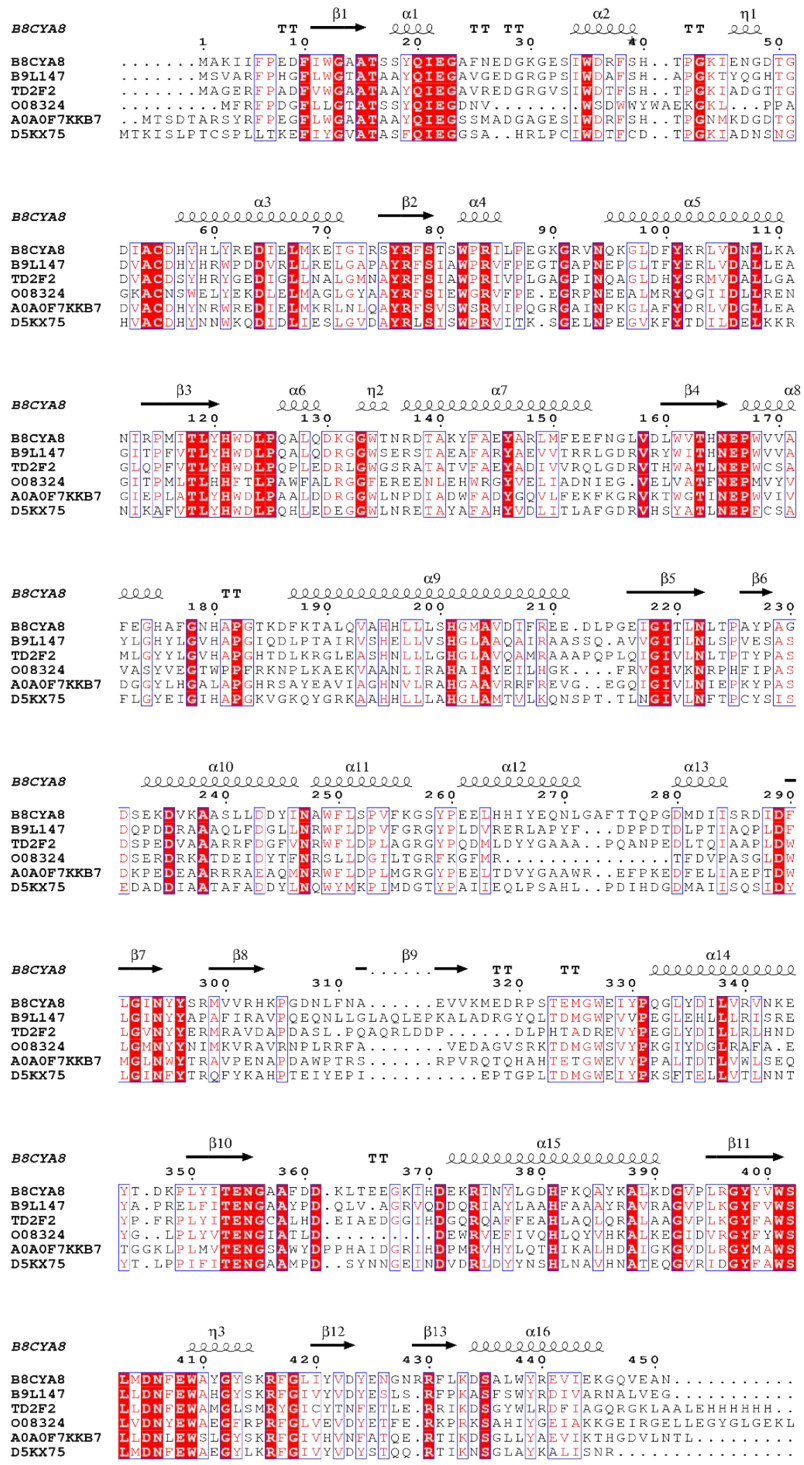

Figure S3. Melting temperature (T_m) of B9L147 in the presence of 0-1M glucose concentrations was measured by Differential Scanning Fluorimetry (DSF) as per the protocol described previously[9,10].

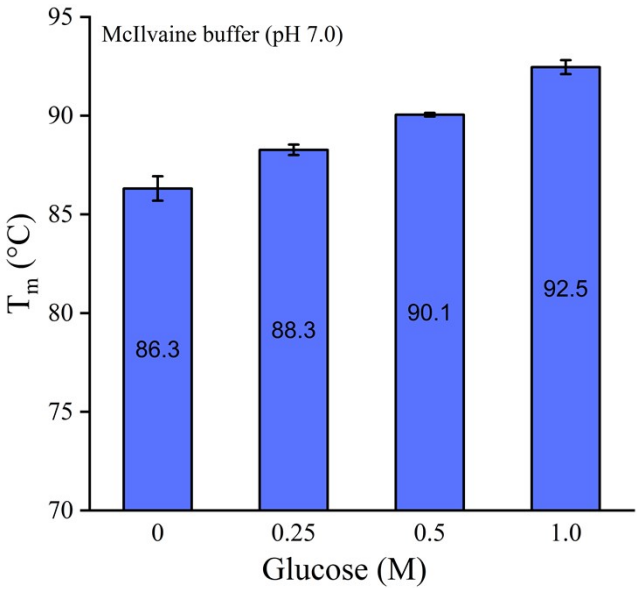

Figure S4. The HPLC analysis of the product generated by B9L147 on the substrate, cellobiose, and without the addition of glucose under the optimum reaction condition described in the method section.

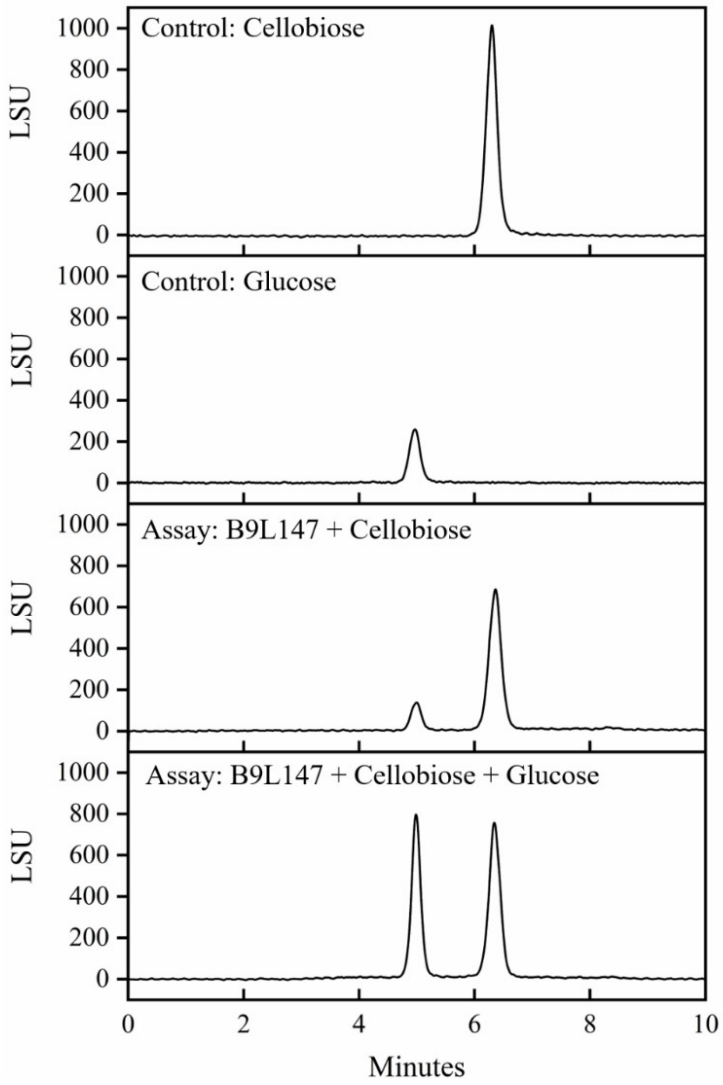

Figure S5. The three-dimensional cartoon representation of the B9L147 model structure with a typical $(\alpha/\beta)_8$ TIM barrel fold. The two catalytic residues (E166 and E357) are located at the fourth and seventh β-strand. The details of the structure generation are mentioned in the material and methods section of the SI.

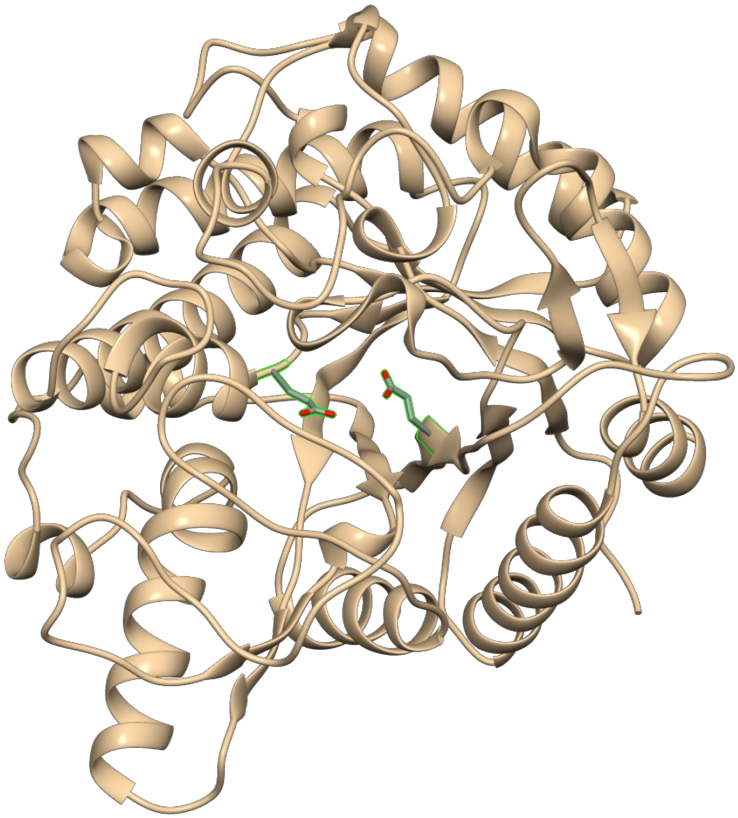

Figure S6. Cartoon representation of the size difference in the capping loop of BGs. We chose three glucose tolerant BG's structure, Chain A of 4PTX from *Halothermothrix orenii*[4], 3WH5 of TD2F2 from metagenome[5]. The yellow regions are catalytic tunnels, while the blue loop is a capping loop of the tunnel that regulates substrate influx and can act as a barrier between the catalytic tunnel environment and outside.

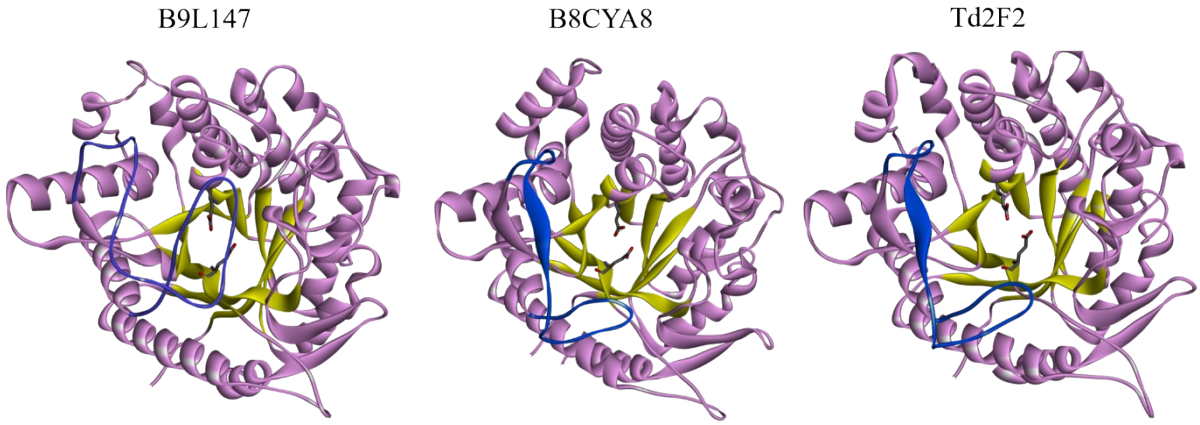

Figure S7. a) B9L147 glucose tolerance in HEPES buffer (pH 7.0) and seawater (pH 8.1) at 84 ℃ (20 mM *p*NPGlc), b) Michaelis-Menton kinetics plot of B9L147 in HEPES buffer (pH 7.0) and seawater (pH 8.1) at 84 ℃. All the assays were done in triplicate, and error bars indicate standard deviation.

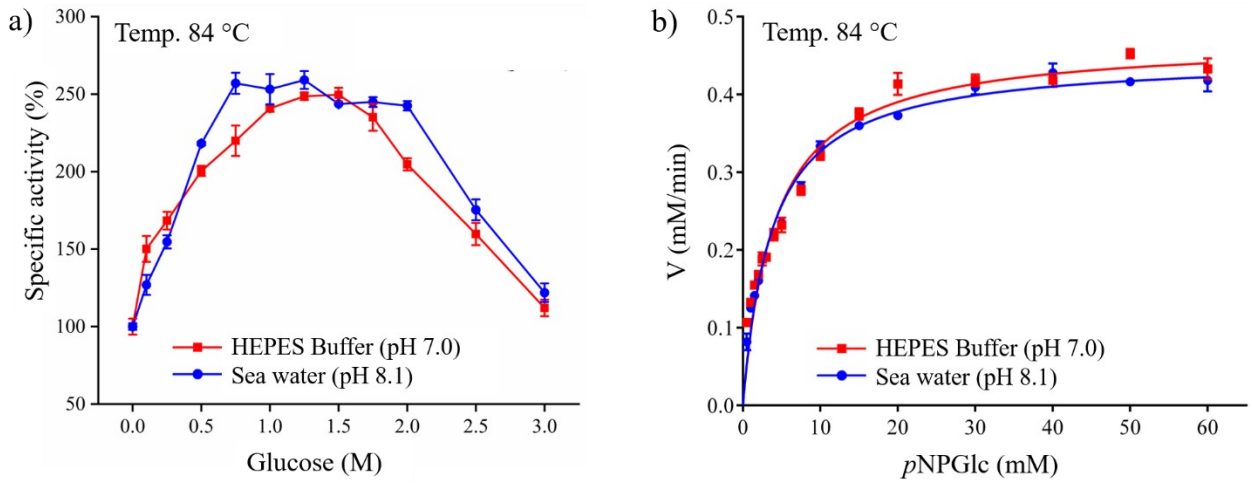

Figure S8. The effect of seawater on the specific activity of a) commercial cellulase mix Cellic CTec2 on substrate Avicel (5 % w/v) at 50 °C, the amount of generated reducing sugars was analyzed by DNS assay. b) commercial almond BG at 37 °C, using *p*NPGlc (20 mM). To compare with the specific activity in seawater, control reactions in McIlvaine buffer, pH 5.0 and 7.0, and pH adjusted seawater, pH 5.0 were used.

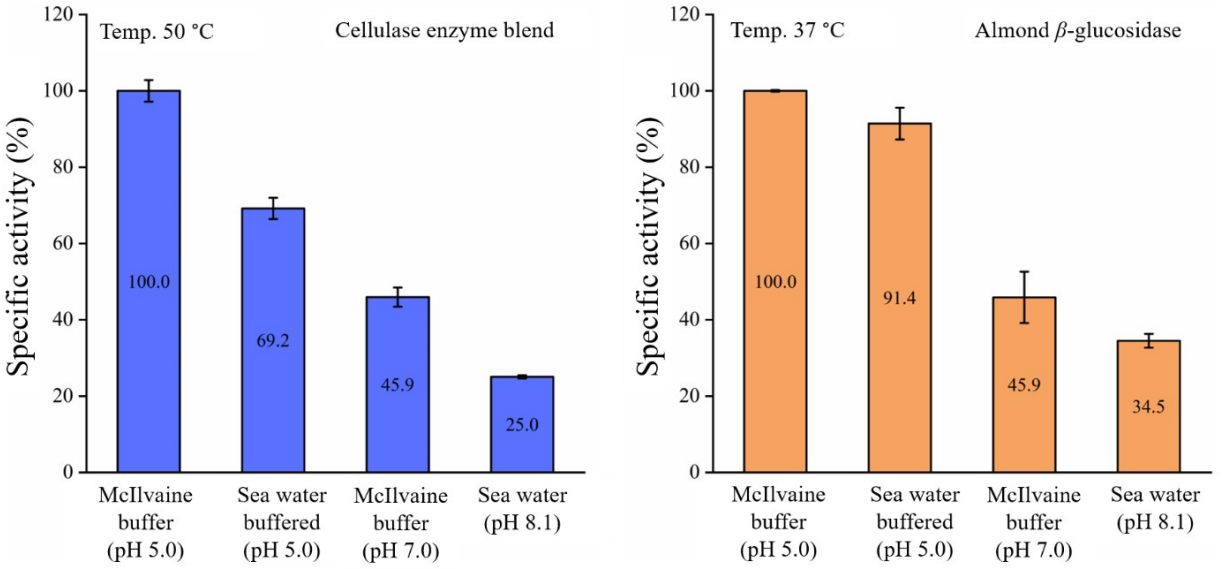

Figure S9. A comparison of electrostatic surface charge distribution of B9L147 with other glucose tolerant β-glucosidase proteins. Both front and back views are shown. The positive potential is highlighted in blue and negative in red. The structures of *β*-glucosidase Td2F2[5] (PDB ID: 3WH5), B8CYA8[11] (PDB ID: 4PTX) and P22505[12] (PDB ID: 2O9P) were taken from PDB database[13].

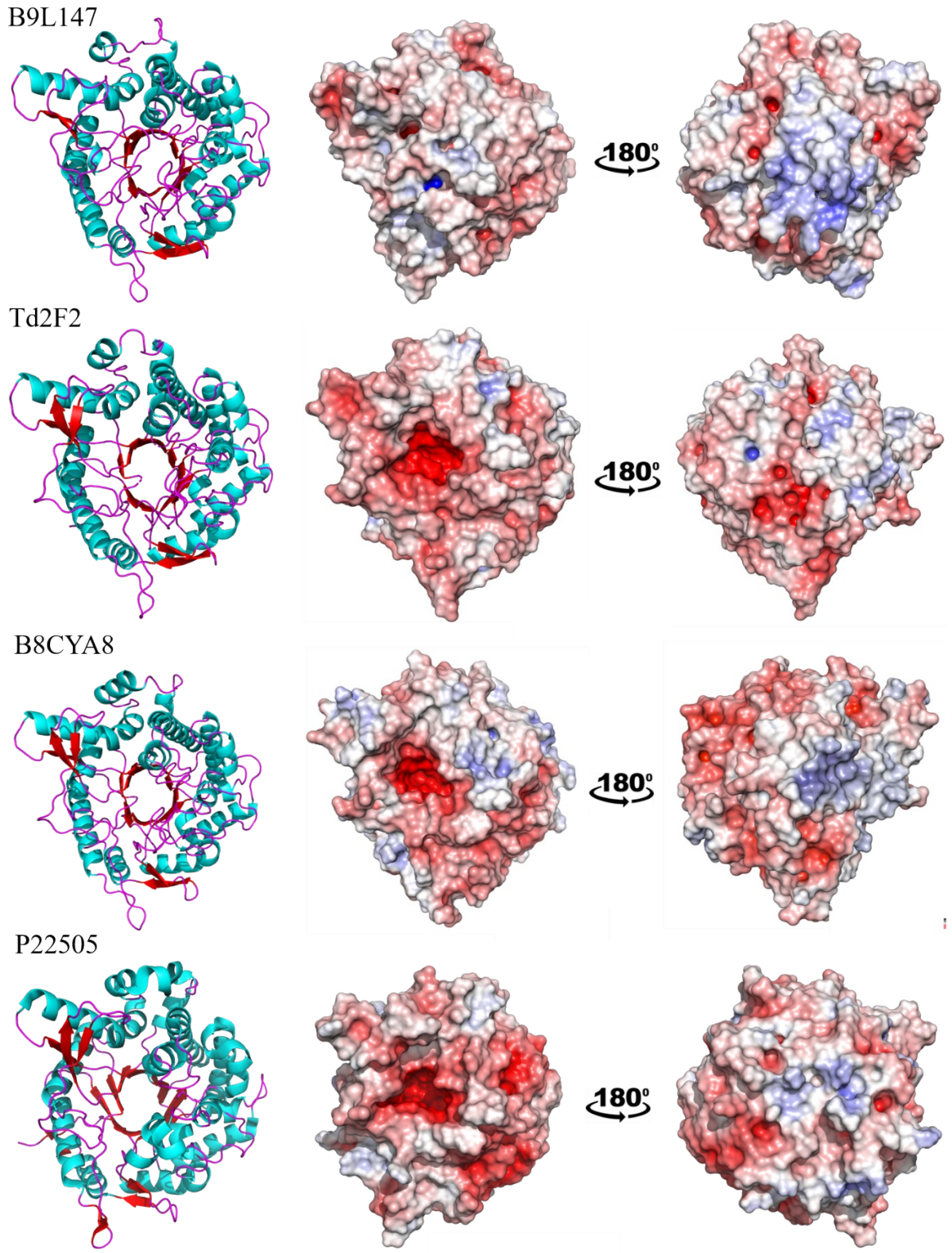

Figure S10. Comparison of the glucose generated by supplementation of β-glucosidase on the synergistic action of endo-1,4-β-D-glucanase from *Acidothermus cellulolyticus* and Cellobiohydrolase I from *Hypocrea jecorina.* Performance of control *β*-glucosidase from almond, B9L147, and B9L147_V169C (V169C in the figure) was evaluated by measuring the amount of glucose generated by the synergistic action of cellulase on Avicel. The reaction was performed in McIlvaine buffer of pH 5.0 and pH adjusted seawater of pH 5.0 at 50 °C. The final product glucose generation was calculated by GOD-POD assay. Our results show that the improvements in the amount of glucose produced.

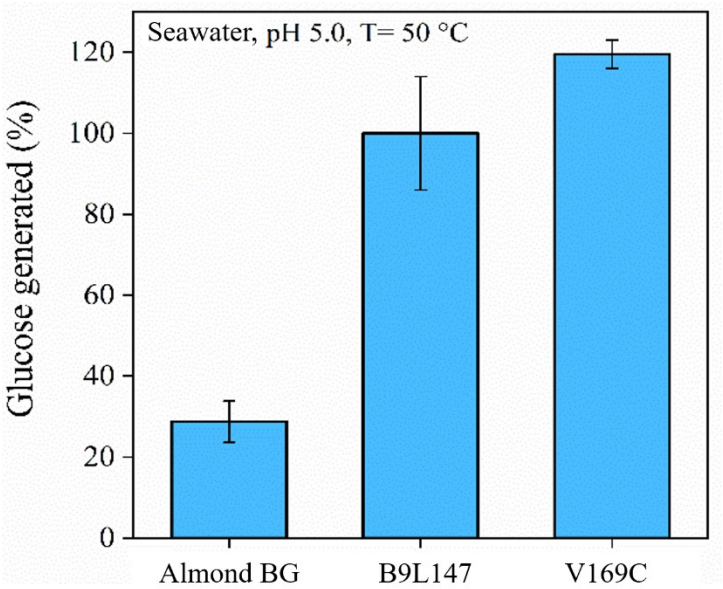

Figure S11. a) Effect of seawater (pH 8.1) on the specific activity of β-glucosidase present in commercial cellulase Cellic CTec2 at 50 °C, using *p*NPGlc (20 mM). For comparison, its specific activity in McIlvaine buffer of pH 5.0 was taken as 100 %. b) Effect of increasing glucose concentration on the specific activity of β-glucosidase present in Cellic CTec2 at its T_{opt} 50 °C McIlvaine buffer of pH 5.0 using *p*NPGlc (20 mM).

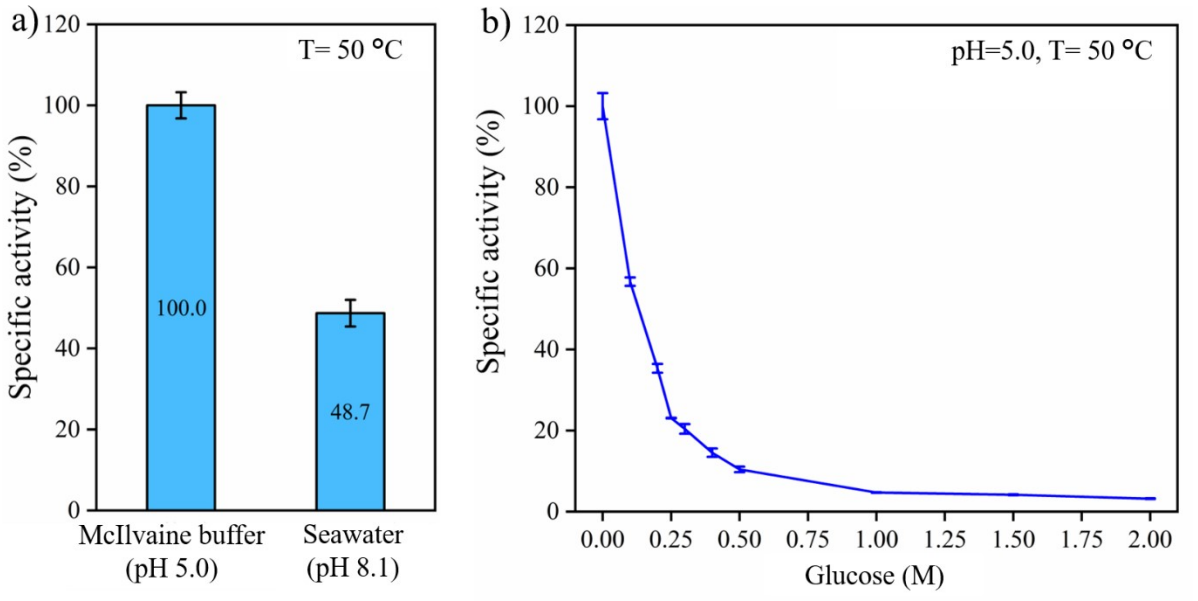

Table S1. The specific activity of B9L147 on chromogenic trisaccharide substrates (10 mM) at 84°C, McIlvaine buffer, pH 7.0.

Trisaccharide substrates (10 mM)	Specific activity (μmol.min^{-1}.mg^{-1})
*p*NPClb	18.0 ± 0.7
*p*NPLac	105.2 ± 2.7
*p*NPMal	11.1 ± 1.0

Table S2: List of salt-tolerant β-glucosidase reported in the literature.

Organism	T_{opt} (°C)	Salt	Stimulation	Tolerance	K_m (mM)	k_{cat} (s^{-1}) or Sp. activity	Ref.
Streptomycete sp.	45	NaCl	0.5 M (1.6-fold)	5 M	10.9	24.1 (μmol min^{-1} mg^{-1})	[14]
Aspergillas niger	70	NaCl	4 M (1.44-fold)	5 M	20.1	20.51 (μmol min^{-1} mg^{-1})	[15]
Thermococcus sp.	78	NaCl, KCl	1.5 M (1.2-fold)	5 M	7.6	195.0 (s^{-1})	[6]
Bacillus cellulosilyticus	40	NaCl	0.2 M (1.2-fold)	1 M	3.0	208.8 (s^{-1})	[16]
Soil Metagenome	50	NaCl	0.02 M (1.35-fold)	0.6 M	2.1	183.9 (μmol min^{-1} mg^{-1})	[17]
Thermobifida halotolerans	45	NaCl	NA	0.05 w/v	22.0	41.8 (s^{-1})	[18]
Bacillus sp.	40	NaCl	15 % (3.3-fold)	30 %	5.4	3.2 (nmol min^{-1} mg^{-1})	[19]
Thermomicrobium roseum	84	NaCl, KCl	No stimulation	1.5 M	3.6	280.7 ± 10.5 (s^{-1})	This study

Table S3. Effect of metal ions on B9L147 specific activity at 84°C, HEPES buffer pH 7.0 on 20 mM *p*NPGlc.

Metal ions	Specific activity (%)	
	5 mM	10 mM
Na^{+}	102.6 ± 3.6	96.9 ± 2.5
K^{+}	101.3 ± 0.8	102.4 ± 2.7
Mg^{2+}	92.6 ± 1.8	94.1 ± 1.7
Mn^{2+}	100.3 ± 2.2	103.5 ± 6.5
Cu^{2+}	93.9 ± 2.3	90.6 ± 2.8

References

1 R. A. Laskowski, M. W. MacArthur, D. S. Moss and J. M. Thornton, *J. Appl. Crystallogr.*, 1993, **26**, 283–291.

2 M. Wiederstein and M. J. Sippl, *Nucleic Acids Res*, 2007, **35**, 407–410.

3 X. Robert and P. Gouet, *Nucleic Acids Res*, 2014, **42**, W320–W324.

4 N. Hassan, T.-H. Nguyen, M. Intanon, L. D. Kori, B. K. C. Patel, D. Haltrich, C. Divne and T. C. Tan, *Appl. Microbiol. Biotechnol.*, 2015, **99**, 1731–1744.

5 T. Uchiyama, K. Miyazaki and K. Yaoi, *J. Biol. Chem.*, 2013, **288**, 18325–18334.

6 S. K. Sinha and S. Datta, *Appl. Microbiol. Biotechnol.*, 2016, **100**, 8399–8409.

7 L. C. Cao, Z. J. Wang, G. H. Ren, W. Kong, L. Li, W. Xie and Y. H. Liu, *Biotechnol. Biofuels*, 2015, **8**, 1–12.

8 Z. Fang, W. Fang, J. Liu, Y. Hong, H. Peng, X. Zhang, B. Sun and Y. Xiao, *J. Microbiol. Biotechnol.*, 2010, **20**, 1351–1358.

9 S. K. Sinha and S. Datta, *Appl. Microbiol. Biotechnol*, 2016, **100**, 8399–8409

0 F. H. Niesen, H. Berglund and M. Vedadi, *Nat. Protoc*, 2007, **2**, 2212–2221.

11 N. Hassan, T. H. Nguyen, M. Intanon, L. D. Kori, B. K. C. Patel, D. Haltrich, C. Divne and T. C. Tan, *Appl. Microbiol. Biotechnol.*, 2015, **99**, 1731–1744.

12 P. Isorna, J. Polaina, L. Latorre-García, F. J. Cañada, B. González and J. Sanz-Aparicio, *J. Mol. Biol.*, 2007, **371**, 1204–1218.

13 H. M. Berman, T. Battistuz, T. N. Bhat, W. F. Bluhm, P. E. Bourne, K. Burkhardt, Z. Feng, G. L. Gilliland, L. Iype, S. Jain, P. Fagan, J. Marvin, D. Padilla, V. Ravichandran, B. Schneider, N. Thanki, H. Weissig, J. D. Westbrook and C. Zardecki, *Acta Crystallogr. Sect. D Biol. Crystallogr.*, 2002, **58**, 899–907.

14 Z. Mai, J. Yang, X. Tian, J. Li and S. Zhang, *Appl. Biochem. Biotechnol.*, 2013, **169**, 1512–1522.

15 L.-N. Cai, S.-N. Xu, T. Lu, D.-Q. Lin and S.-J. Yao, *J. Biotechnol.*, 2019, **292**, 12–22.

16 J. Wu, A. Geng, R. Xie, H. Wang and J. Sun, *Int. J. Biol. Macromol.*, 2018, **109**, 872–879.

17 J. Lu, L. Du, Y. Wei, Y. Hu and R. Huang, *Acta Biochim. Biophys. Sin. (Shanghai).*, 2013, **45**, 664–673.

18 Y. R. Yin, P. Sang, M. Xiao, W. D. Xian, Z. Y. Dong, L. Liu, L. Q. Yang and W. J. Li, *Biomass Convers. Biorefinery*, 2021, **11**,1245–1253.

19 J. M. i. Lee, Y. R. Kim, J. K. yu. Kim, G. T. Jeong, J. C. Ha and I. S. Kong, *Bioprocess Biosyst. Eng.*, 2015, **38**, 1335–1346.